# STRUCTURE AND PROPERTIES OF A POWDER METALLURGY Al-Zr-Ti ALLOY

PŘEMYSL MÁLEK[1]*, MILOŠ JANEČEK[1], PAVEL BARTUŠKA[2]

A good high-temperature stability of microstructure and strength has been recently found in Al-1.25at.%(Zr+Ti) alloys rapidly solidified using the chill block melt spinning method. In order to prepare a bulk material an alternative processing route consisting of high-energy gas atomisation and suitable consolidation was chosen. The supersaturation of the matrix of the consolidated material by Zr and Ti atoms was significantly lower than that in the melt spun ribbons of the same material. No fan-shaped configuration of the $L1_2$ modification of the $Al_3(Zr_xTi_{1-x})$ phase was observed in the consolidated materials and, therefore, the microhardness in both as-received and aged states was significantly lower than that of the as-melt spun material. The long term stability of the microhardness is similar in both types of material.

K e y w o r d s: Al-1.25at.%(Zr+Ti) alloys, gas atomisation, chemical and phase composition, microstructure, microhardness, tensile tests

# STRUKTURA A VLASTNOSTI SLITINY Al-Zr-Ti PŘIPRAVENÉ METODOU PLYNNÉ ATOMIZACE

Slitiny Al-1,25at.%(Zr+Ti) připravené nástřikem taveniny na rotující měděný válec se vyznačují dobrou stabilitou struktury a pevnosti u zvýšených teplot. Pro přípravu objemového materiálu byla použita alternativní metoda vysokoenergetické plynné atomizace následované zhutněním. Přesycení matrice zhutněného materiálu atomy Zr a Ti je výrazně nižší než v nastříkaných páscích. Nebyla pozorována vějířovitá precipitace metastabilní $L1_2$ modifikace fáze $Al_3(Zr_xTi_{1-x})$ a mikrotvrdost zhutněného materiálu jak ve výchozím stavu, tak po stárnutí u zvýšených teplot byla nižší než v páscích. Dlouhodobá stabilita struktury a pevnosti byla v obou typech materiálu obdobná.

[1] Department of Metal Physics, Charles University, Ke Karlovu 5, 12116 Prague 2, Czech Republic
[2] Institute of Physics, Academy of Sciences of the Czech Republic, Na Slovance 2, 18040 Prague 8, Czech Republic
* corresponding author, e-mail: malek@met.mff.cuni.cz

## 1. Introduction

Current age hardenable aluminium alloys cannot be used for elevated temperature applications as any exposition to temperatures exceeding about 423 K results in a drop of their strength. In order to develop Al-based alloys with a stable high strength at elevated temperatures, the alloys of new compositions have to be designed. These alloys must contain a high volume fraction of small particles that are resistant both to dissolution and coarsening. Suitable additives for such alloys have to meet the following requirements:

– a capability to form intermetallic phases of a low lattice mismatch to the Al-matrix,

– a low equilibrium solid solubility up to temperatures of 700 K in order to prevent the dissolution of strengthening phases,

– a low diffusivity in Al in order to slow down the diffusion controlled coarsening of strengthening particles.

Zirconium meets very well all these requirements – it is able to form the $Al_3Zr$ phase with a very low lattice mismatch to the Al-based matrix [1, 2], its maximum solid solubility reaches only 0.28 wt.% at 934 K [3], and its diffusion rate in Al is the slowest one of all transition metals [4]. The $Al_3Zr$ phase appears in two modifications – the formation of the equilibrium phase with a tetragonal $DO_{23}$ structure and a lattice mismatch to Al-matrix of about 2.9 % [1] is preceded by the formation of the metastable phase with a cubic $L1_2$ structure and even smaller lattice mismatch (about 0.7 % [2]). According to the theory of diffusion-controlled particle coarsening, its rate decreases with decreasing lattice mismatch to the matrix [5, 6]. Therefore, metastable $Al_3Zr$ phase should be more resistant to coarsening than the equilibrium phase. Moreover, the particle size of the metastable $Al_3Zr$ phase is usually significantly lower, which should result in a higher strengthening effect.

Ternary additives as V, Hf or Ti [7, 8] may further reduce the low lattice mismatch of both modifications of the $Al_3Zr$ phase. Recently, it has been shown in several papers that e.g. Ti atoms may substitute for Zr atoms in the lattice of the $Al_3Zr$ phase and reduce its lattice mismatch even to zero in case of a suitable Zr : Ti ratio [4, 9]. Consequently, even stronger resistance to particle coarsening may be expected in this ternary Al-Zr-Ti alloy [7, 10].

Conventional ingot metallurgy processing route results in massive segregation and formation of coarse primary particles so that the desired structure with a homogeneous distribution of small second phase particles cannot be formed. On the other hand, rapid solidification techniques with quenching rates up to $10^6$ $K \cdot s^{-1}$ successively extend the solid solubility limits, suppress the formation of primary particles, and homogenise and refine the solidified structure [11]. The desirable distribution of second phase particles can be then formed through the decomposition of the supersaturated matrix during the subsequent annealing.

The Al-Zr-Ti alloys containing 5 vol.% of the $Al_3(Zr_xTi_{1-x})$ particles in fully precipitated state ($x$ ranging from 0 to 1) prepared using melt-spinning method were previously studied [12–15]. A strengthening effect measured by Knoop microhardness (HK) testing was found in all Zr containing materials at temperatures above 600 K. The HK peak shifts to higher temperatures with increasing Ti:Zr ratio and the best combination of HK value and its high temperature stability was found in alloys with stoichiometric parameters $x = 0.5$ and 0.75. These alloys exhibited an increase in HK during long-term annealing at 600 K, while a gradual drop in HK was observed during annealing at higher temperatures (Fig. 1).

As the shape of melt-spun ribbons is not convenient for technical applications, an alternative processing route represented by modern powder metallurgy was chosen. High-energy gas atomisation method is characterised by cooling rates between $10^4$ and $10^5$ $K \cdot s^{-1}$ that should ensure all benefits of rapid solidification in the powder material produced. A problem arises during consolidation of powders to a bulk material. In order to achieve the necessary material integrity, relatively high temperatures are necessary. On the other hand, the consolidation temperature must not be too high in order to retain all beneficial properties of rapidly solidified products.

The Al-Zr-Ti alloy prepared using powder metallurgical route was studied in the present work. The attention was paid to the microstructure and mechanical properties both of powder and consolidated material. The ageing of these materials at elevated temperatures was compared with the melt-spun material.

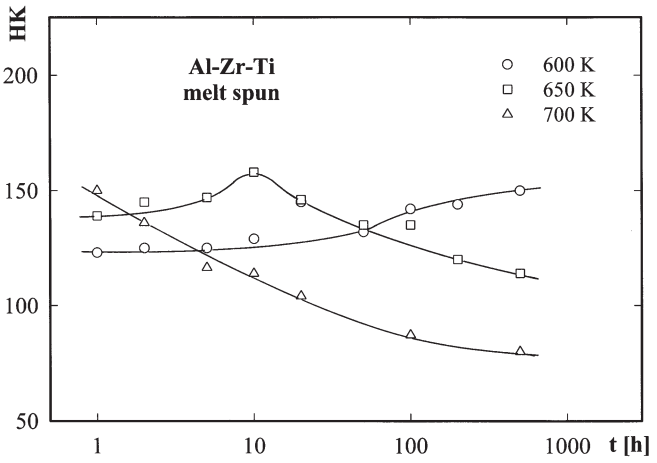


Fig. 1. The influence of long-term annealing on the Knoop microhardness of the as-melt spun Al-$Al_3(Zr_{0.5}Ti_{0.5})$ alloy [15].

## 2. Experimental material and procedure

A nominal chemical composition Al-1.25at.%(Zr+Ti) was selected that corresponds to a phase composition of Al-5vol.%$Al_3(Zr_xTi_{1-x})$ in a fully precipitated state (supposing a negligible equilibrium solid solubility of Zr and Ti in Al). The stoichiometric parameter $x$ was selected from the range between 0.5 and 0.75. The 99.995 % Al, Al-6wt.%Zr, and Al-10wt.%Ti master alloys were remelted in silica crucibles of the high-energy gas atomiser PSI HERMICA 10/21 VI at 1173 K. The melt was atomised with argon and passivated in two steps in order to achieve a controlled oxidation. About 90 % of powder particles have the size below 100 $\mu$m and the maximum of the particle size distribution lies at about 65 $\mu$m (Fig. 2). The powder was sieved and the fraction finer than 100 $\mu$m was encapsulated in aluminium cans, precompacted, degassed, and hot extruded at 623 or 673 K. The extrusion ratio was 25:1 and the diameter of the resulting bar was about 12 mm.

The chemical composition of consolidated material was studied using the X--ray microanalyser JEOL Superprobe 733. The analyses were performed on the metallographically polished sections parallel to the extrusion direction. Both area and point analyses were carried out at different places in order to control the homogeneity in distribution of individual additives. The mean composition determined from more than 150 area analyses is given in Table 1. The sum of Zr and Ti content is 1.2 at.%, i.e. very close to the nominal composition 1.25 at.%.

On the mesoscale level, the structure of the powder material was studied using optical microscope Olympus IX-70 BF equipped with a digital camera Olympus. The Dix-Keller etchant was used for the development of the as received structure. The structure of the consolidated material was studied using transmission electron

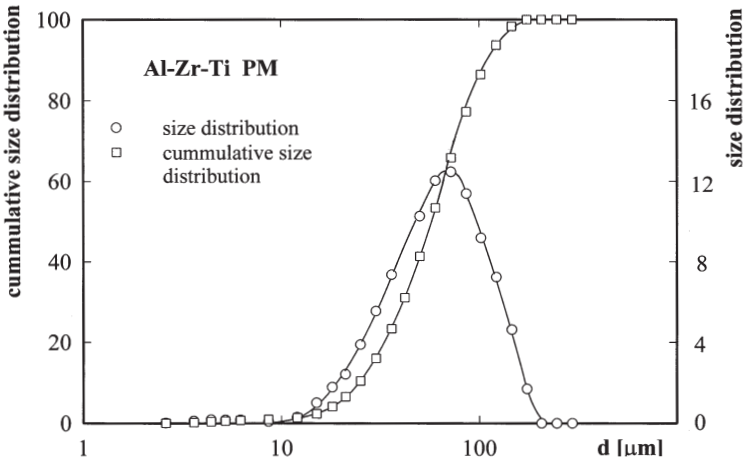


Fig. 2. The size distribution of the as-atomised powder particles.

Table 1. The chemical composition of the Al-Zr-Ti alloy

| Solute | Content in wt.% | Content in at.% |
|---|---|---|
| Zr | 2.6 | 0.79 |
| Ti | 0.7 | 0.41 |

microscopy. The discs parallel to the extrusion direction were thinned electrolytically in the 66 % $HNO_3$ – 33 % $CH_3OH$ solution and observed using the JEOL 2000 FX microscope at 200 kV. Electron diffraction experiments were performed in order to identify the structure of present particles.

Both powder and consolidated material were annealed under argon protective atmosphere for various times at temperatures up to 773 K. The Vickers microhardness was measured using LECO M-400 A microhardness tester with the load of 10 g and dwell time of 15 s.

Tensile samples of a round cross section (about 6 mm in dia) were cut from the consolidated material extruded at 623 K parallel to the extrusion direction and annealed for 100 hours at temperatures of 600, 650, and 700 K. The tensile tests were performed at 295 K and strain rate of $4 \times 10^{-4}$ $s^{-1}$ using INSTRON 1195 testing machine. The strain rate sensitivity parameter $m$ $(= \partial \log \sigma / \partial \log \dot{\varepsilon})$ was determined by the strain rate change method.

## 3. Experimental results

### 3.1 Microstructure and composition of the as-received material

The microstructure and composition inhomogeneity represents frequently a serious problem in rapidly solidified materials. The microstructure of melt-spun ribbons depends generally on the distance from the chilled (contact) surface [12] whereas the microstructure of a powder material depends strongly on the size of powder particles. Fig. 3 shows clearly a coarser solidification structure in larger powder particles. No information is available about the phase composition of individual powder particles.

The bulk material was processed by the consolidation of powder particles with a broad size distribution. Therefore, a composition and microstructure inhomogeneity may be also expected in the bulk material. EDX analyses showed a great inhomogeneity in the distribution of both Zr and Ti within the extruded material. In area analyses performed at the magnification of 20000 (diameter of the corresponding area about 3 $\mu$m), the Zr content was found between 1.6 and 4.0 wt.% with the mean value of about 2.6 wt.% and the Ti content between 0.4 and 1.1 wt.% with the mean value of about 0.7 wt.%. One may assume that this large scatter in Zr and Ti contents reflects the presence of precipitates that were really observed

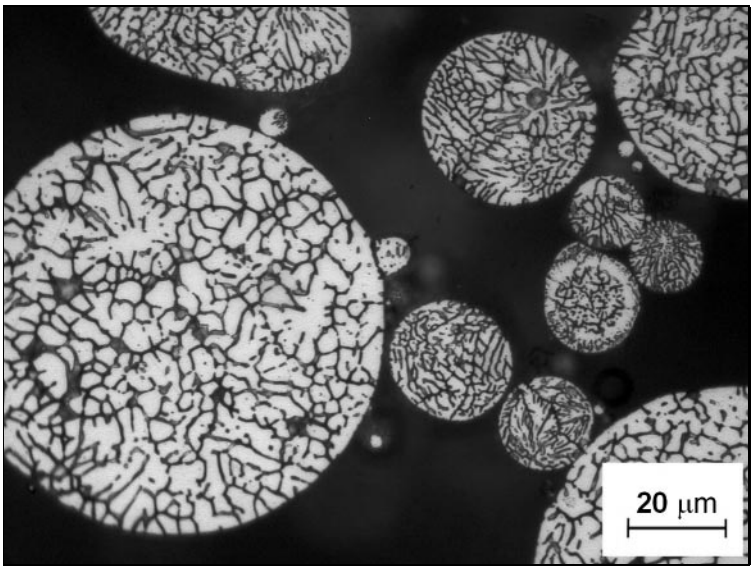


Fig. 3. The solidification structure of the as-atomised powder particles, light microscopy.

in back scattered electron image. In order to verify this hypothesis, a number of point analyses with much smaller analysed area was performed. At places where the precipitates are located the analyses confirmed higher Zr and Ti contents (Zr up to 14 wt.% and Ti up to 4 wt.%) whereas a very low content of Ti in the matrix was found. The ratio of Zr and Ti content in all analyses was close to 3.7 in wt.%, which corresponds to the ratio of 1.9 in at.%. Supposing a fully precipitated state the corresponding stoichiometric parameter $x$ is 0.66, i.e. it lies in the optimum range.

The microstructure of the material extruded at 623 K exhibits directionality – individual grains are elongated and arranged into bands parallel to the extrusion direction (Fig. 4). The grain size ranges between 1 and 2 $\mu$m along the transversal direction and up to 5 $\mu$m in the longitudinal direction. Numerous particles of various sizes and shapes are present in the microstructure. The typical particles are coarse, nearly round (marked A) and cylindrical particles (marked B) of the size comparable with the grain size and contain a large amount of Fe. Other particles (marked C) of a rectangular cross section are finer and contain Zr and Ti. Electron diffraction analysis revealed that these particles were formed by the metastable $Al_3$(Zr,Ti) phase of the $L1_2$ structure type. A very similar structure was found in the material extruded at the temperature of 673 K (Fig. 5). Some interfaces,

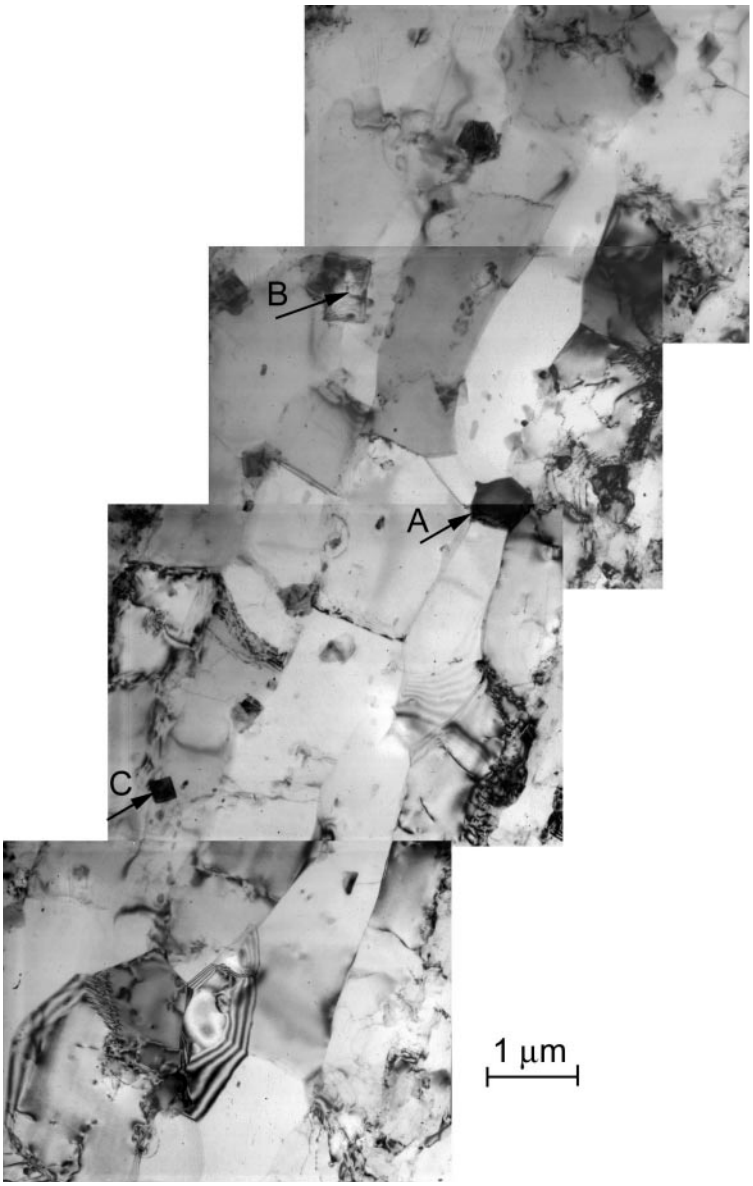


Fig. 4. The microstructure of the powder material extruded at 623 K, TEM.

especially those perpendicular to the extrusion direction, are formed by dislocation arrays and have, therefore, a character of subboundaries.

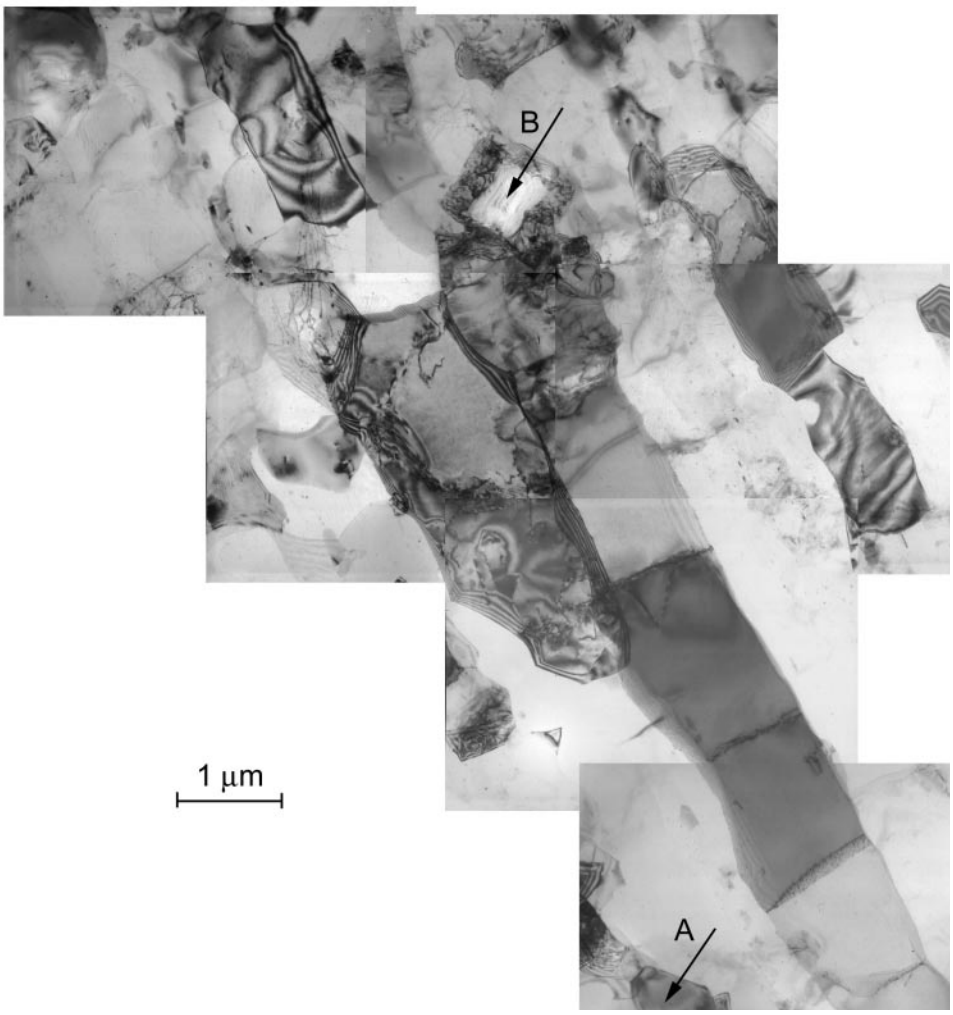


Fig. 5. The microstructure of the powder material extruded at 673 K, TEM.

### 3.2 The ageing at elevated temperatures

The influence of ageing on the Vickers microhardness was studied both in the powder and in extruded materials. The isochronal annealing curve of microhardness (annealing time of 1 hour) of the as-atomised powder material exhibits a peak after annealing at 673 K. Further increase in annealing temperature results in a drop of the microhardness (Fig. 6). A large scatter in measured HV values is a

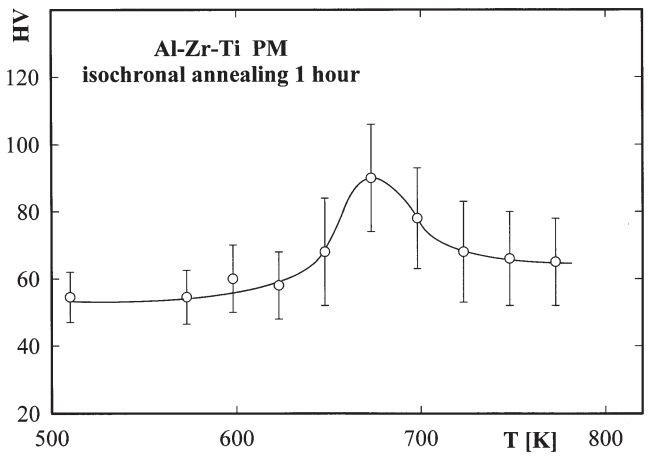


Fig. 6. The isochronal annealing curve of microhardness of the as-atomised powder material.

Table 2. Vickers microhardness of the powder material after isothermal annealing

| Annealing temperature/annealing time | 1 hour | 10 hours | 100 hours |
|---|---|---|---|
| 650 K | 70 ± 18 | 83 ± 16 | 83 ± 13 |
| 700 K | 78 ± 16 | 73 ± 15 | 71 ± 13 |

typical feature of the as-atomised powder material and reflects probably a broad variety of microstructure in individual powder particles. Higher HV values were generally found in smaller powder particles with a finer microstructure. The as--atomised powder material exhibits a good long-term stability of microhardness during annealing at 650 K and a slow softening during annealing at 700 K (Table 2).

Similar experiments were carried out in the powder material extruded at 623 and 673 K. Table 3 shows that the microhardness of extruded materials is significantly higher than that of the powder material and the scatter of measured experimental values is much lower. Similarly to the as-atomised powder material, a strengthening effect and a good long term stability were observed at temperatures 600 and 650 K whereas an overageing occured at 700 K.

The influence of annealing at elevated temperatures was also studied using tensile tests. Important deformation characteristics of the material extruded at 623 K are summarised in Table 4. Identical results (within the experimental scatter) were obtained after extrusion at 673 K. Fig. 7 shows the true stress vs. true strain curves of the material extruded at 623 K. The ductility was found to be nearly independent of the thermal treatment. An age hardening effect was observed at

Table 3. Vickers microhardness of the extruded materials measured on transversal section after thermal treatment

| Treatment/material | Extruded at 623 K | Extruded at 673 K |
|---|---|---|
| As-extruded | 95 ± 10 | 101 ± 8 |
| Annealed 600 K/100 h | 118 ± 6 | 112 ± 4 |
| Annealed 650 K/10 h | 114 ± 5 | 110 ± 7 |
| Annealed 650 K/100 h | 112 ± 6 | 103 ± 4 |
| Annealed 700 K/10 h | 94 ± 5 | 82 ± 8 |
| Annealed 700 K/100 h | 91 ± 4 | 80 ± 8 |

Table 4. Deformation characteristics of the material extruded at 623 K after thermal treatment

| Treatment | $R_p0.2$ [MPa] | $R_m$ [MPa] | $\sigma_{max}$ [MPa] | $A$ [%] | $n$ | $m$ |
|---|---|---|---|---|---|---|
| As-extruded | 257 | 274 | 294 | 18 | 0.025 | 0.08 |
| Annealed 600 K/100 h | 286 | 300 | 326 | 21 | 0.03 | 0.09 |
| Annealed 650 K/100 h | 258 | 281 | 305 | 19 | 0.04 | 0.08 |
| Annealed 700 K/100 h | 189 | 227 | 251 | 21 | 0.075 | 0.06 |

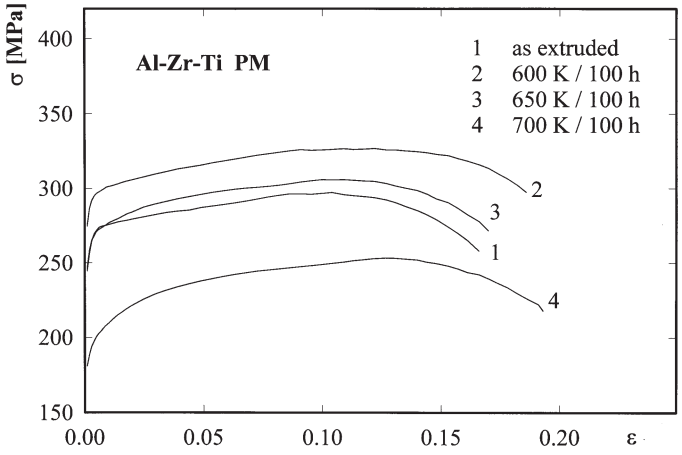


Fig. 7. The true stress vs. true strain curves of the powder material extruded at 623 K.

temperatures of 600 and 650 K and an overageing effect at 700 K. All curves exhibit a strain hardening region at elongation below about 12 %. The flow stress decrease observed at higher strains results probably from the necking of tensile samples.

The strain hardening can be quantitatively described by a simple relationship

$$\sigma = K_1 \varepsilon^n, \tag{1}$$

where $K_1$ is an empirical constant and $n$ is a strain-hardening exponent that may be evaluated as a slope of the $\ln \sigma$ vs. $\ln \varepsilon$ plot. Fig. 8 shows a good linearity of these plots for each thermal treatment and an increase in strain hardening exponent $n$ with increasing annealing temperature.

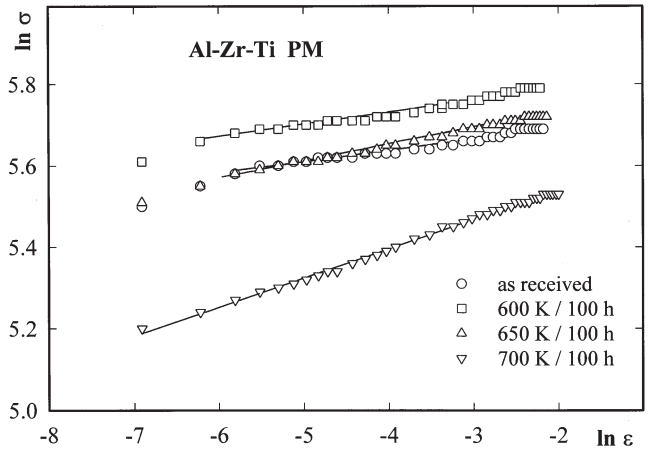


Fig. 8. The $\ln \sigma$ vs. $\ln \varepsilon$ plots of the powder material extruded at 623 K.

Fine-grained materials exhibit frequently a strong strain rate sensitivity and their behaviour can be described by a relationship

$$\sigma = K_2 \dot{\varepsilon}^m, \tag{2}$$

where $K_2$ is an empirical constant and $m$ is a strain rate sensitivity parameter. The parameter $m$ was evaluated from the strain rate changes (with a ratio 10:1) performed at each sample at an elongation of about 5 % as

$$m = \ln(\sigma_2/\sigma_1)/\ln(\dot{\varepsilon}_2/\dot{\varepsilon}_1), \tag{3}$$

where $\sigma_2$ and $\sigma_1$ are the flow stresses corresponding to strain rates $\dot{\varepsilon}_2$ and $\dot{\varepsilon}_1$, respectively. The values of the parameter $m$ are low and nearly independent of the thermal treatment.

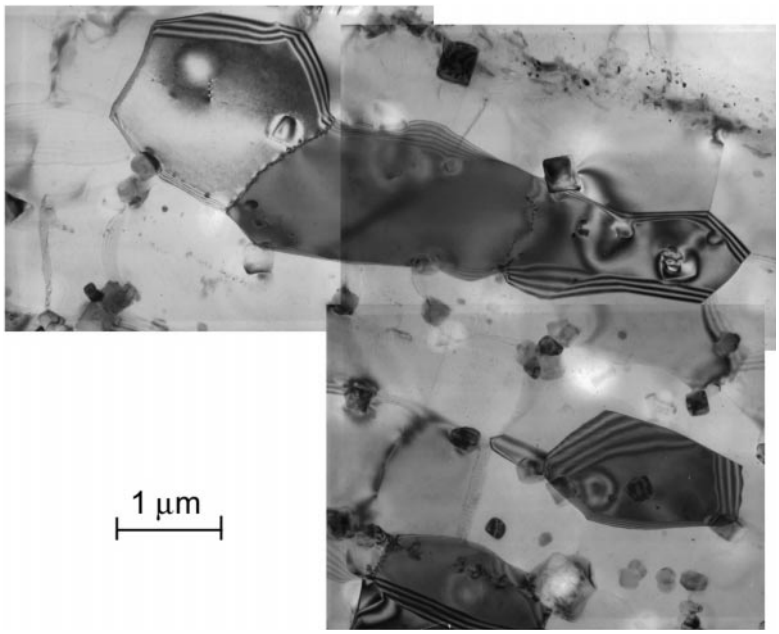


Fig. 9. The microstructure of the extruded powder material after ageing 100 h at 600 K.

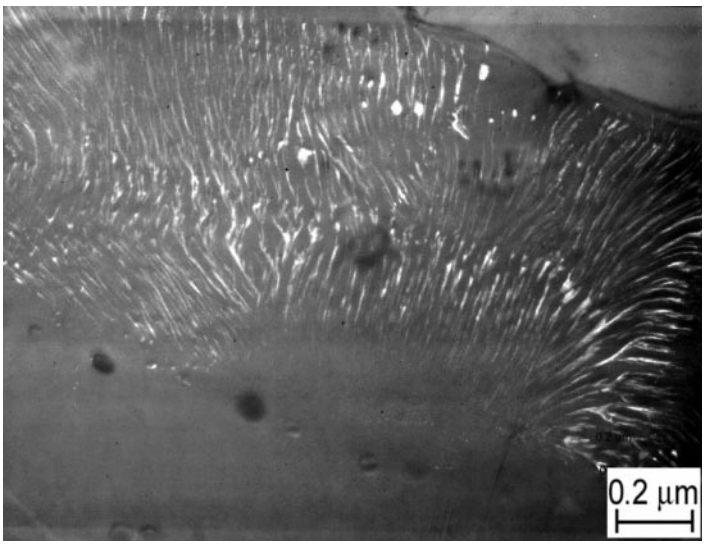


Fig. 10. The fan shaped precipitation in the extruded powder material after ageing 100 h at 600 K.

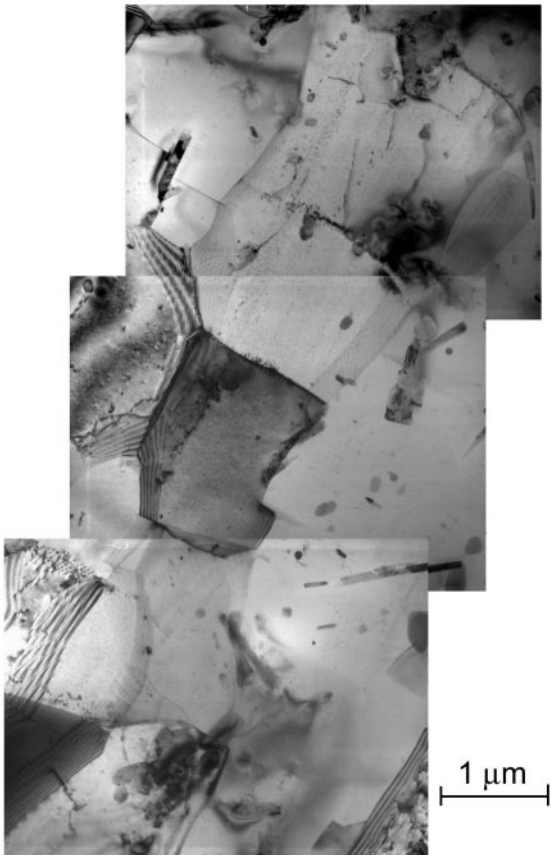


Fig. 11. The needle like precipitation in the extruded powder material after ageing 100 h at 700 K.

The influence of ageing at elevated temperatures on the microstructure of extruded materials was investigated using transmission electron microscopy. The size, shape and arrangement of grains remain unchanged after ageing. The main difference was found in the phase composition. An increase in the volume fraction of rectangular particles in the sample aged at 600 K for 100 hours is documented at the TEM micrographs (Fig. 9). Very fine particles arranged into fans were observed only exceptionally (Fig. 10). Electron diffraction analysis proved that both above-mentioned types of particles were formed by the metastable $Al_3(Zr,Ti)$ phase with the $L1_2$ structure type. Needle-like particles of the stable modification of the $Al_3(Zr,Ti)$ phase with the $DO_{23}$ structure type were found in the sample aged at 700 K for 100 hours (Fig. 11).

## 4. Discussion

### 4.1 The as-received material

A high strength may be reached in Al-based alloys containing a dense distribution of small particles. In case that these particles are formed during ageing a microsegregation free solidification microstructure is the best precursor. However, the problem is how to prepare such a structure in materials where the solute content exceeds significantly the equilibrium solid solubility limit. One of the ways how to prepare such structure is using enhanced solidification rates which result in a non-equilibrium structure. Several processing methods can be taken into account:

– Chill casting is characterised by solidification rates that are not sufficiently high to produce a microsegregation free microstructure in Al-Zr-Ti alloys [16, 17]. Coarse petal-like particles composed of a dendritic structure of the $L1_2$ $Al_3Zr$ or $Al_3Ti$ phases are usually formed [18, 19].

– The melt spinning method characterised by extremely high cooling rates (up to about $10^6$ $K \cdot s^{-1}$) was suggested as a way to a microsegregation free microstructure [11]. The main disadvantage of as-melt-spun materials is their shape which is inconvenient for their further processing to a bulk material.

– High energy gas atomisation might represent a compromise – it produces a powder material that may be easily consolidated. However, the achievable solidification rate is usually several orders lower than that in melt spinning. Moreover, the consolidation occurs at elevated temperatures which might suppress the benefits of rapid solidification.

Our previous investigation of the Al-1.25at.%(Zr+Ti) alloys revealed that even melt spinning is not able to form a completely microsegregation-free microstructure and to retain all solutes in the supersaturated matrix [12, 13]. The particles of the metastable $L1_2$ modification of the $Al_3(Zr_xTi_{1-x})$ phase were found in the as-melt-spun ribbons and their volume fraction was estimated to be about 2 vol.% in alloys with a stoichiometric parameter $x = 0.5$ and 0.75 [12]. Therefore, the presence of primary particles can also be expected in powder material prepared at significantly lower cooling rates. Fig. 3 confirms clearly this expectation. The extrusion of the powder material occurs in the temperature range where age hardening was observed in melt-spun Al-Zr-Ti alloys. New particles can be formed during this processing step and the amount of Zr and Ti atoms that remain dissolved in the matrix of the extruded material is very low (see the results of EDX analysis). One of the main benefits of rapid solidification – an extended solid solubility – is, thus, not reached in our material.

Mechanical properties of the Al-Zr-Ti alloy are influenced not only by the volume fraction of particles, but also by their size. Coarse particles were preferentially formed in the extruded powder material whereas fans of very fine $L1_2$ $Al_3(Zr_xTi_{1-x})$ particles (the size of individual particles of about 10 nm) were

present in the ribbon [13]. The size of these coarse particles is of the order of 100 nm. Many of them are primary particles containing impurities as, e.g., Fe. No fan-shaped precipitation was observed in the as-extruded powder material. The absence of fine particles and a low content of Zr and Ti solutes in the matrix resulted in a very low microhardness of the individual powder particles (HV = 55). This value represents only about 50 % of the value found in melt-spun materials of a similar chemical composition. A microhardness increase in the extruded material to a value comparable with that of the as-melt-spun material (HV close to 100) results partially from a strain hardening and partially from an age hardening occurring during extrusion at elevated temperatures.

### 4.2 Ageing at elevated temperatures

The differences in the phase composition between the melt-spun and powder materials predict the differences in their ageing response. Our previous investigation of the melt-spun Al-1.25at.%(Zr+Ti) ribbons revealed that about 60 % of the Zr and Ti atoms remained in the supersaturated solid solution [12]. These atoms participated then in the precipitation process during annealing at elevated temperatures and isochronal annealing curves of microhardness showed an age hardening effect (peak microhardness of about 150) at temperatures close to 650 K in alloys with higher Zr:Ti ratio [14, 15]. The present experiments revealed that the level of supersaturation of the matrix by Zr and Ti atoms was much lower in the as--atomised powder material. Consequently, very few Zr and Ti atoms were available for precipitation during annealing, and the peak microhardness was significantly lower (about 90) than in the melt-spun material. Further reduction in supersaturation might be expected in the extruded powder material due to the precipitation occurring during extrusion. This effect should be more pronounced at higher extrusion temperature. The microhardness measurements confirmed this assumption. The difference between the microhardness in the peak aged and in the as-extruded state was about 20 after extrusion at 623 K whereas only about 10 after extrusion at 673 K.

The stability of high microhardness during long term ageing (up to 500 h) at 600 K was the most remarkable property of melt-spun alloys with the stoichiometric parameter $x = 0.5$ and 0.75. The precipitation of the metastable $L1_2$ modification of the $Al_3(Zr_xTi_{1-x})$ phase in the fan shaped morphology was responsible for the peak microhardness [15]. The as-atomised and extruded powder materials exhibit a good stability of microhardness even at 650 K as shown in Tables 2, 3. However, the microhardness values are significantly lower than those in the melt-spun materials due to a very rare presence of the strengthening $L1_2$ phase. Similarity in the behaviour of both melt-spun and powder materials was found at 700 K where an

overageing occurred. In both materials this overageing is caused by the transformation of the metastable $L1_2$ to the stable $DO_{23}$ modification of the $Al_3(Zr_xTi_{1-x})$ phase.

The results of tensile tests are qualitatively very similar to those obtained from microhardness measurements. Although both these methods are completely different, a relationship between them is frequently discussed. According to Shaw et al. [20] a simple empirical relationship in the form

$$R_{\mathrm{p}}0.2/\mathrm{HV} = 3.3 \tag{4}$$

is often observed. A more complicated formula taking into account also the strain hardening effect was suggested by Cahoon et al. [21]. In case that the true stress $\sigma$ vs. true strain $\varepsilon$ can be described by formula (1) a relationship between the yield stress and microhardness can be written as

$$R_{\mathrm{p}}0.2/\mathrm{HV} = 3.27(0.1)^n. \tag{5}$$

Alternatively, ultimate tensile strength $R_{\mathrm{m}}$ can be correlated with microhardness values. Tabor [22] suggested a formula

$$R_{\mathrm{m}}/\mathrm{HV} = 3.27(1-n)(12.5/(1-n))^n. \tag{6}$$

As shown in Fig. 8, the requirement of a linear $\ln\sigma$ vs. $\ln\varepsilon$ dependence is met in our materials, and relationships (5) and (6) can be used. In Table 5 the validity of the above relationships is tested. It may be seen that the Tabor's equation [22] gives the best agreement with experimental results.

The microstructure of the extruded powder material was found to consist of fine grains and did not significantly change even after annealing at 700 K. A fine grained microstructure is one of prerequisites of the superplastic behaviour [23] when grain boundaries become the main carriers of deformation and grain boundary

Table 5. The relation between tensile test characteristics and microhardness values according to various theories

| Material | $R_{\mathrm{p}}0.2/\mathrm{HV}$ | | | $R_{\mathrm{m}}/\mathrm{HV}$ | |
|---|---|---|---|---|---|
| | exp | theory [20] | theory [21] | exp | theory [22] |
| As-extruded | 2.8 | 3.3 | 3.1 | 3.1 | 3.1 |
| Annealed 600 K/100 h | 2.5 | 3.3 | 3.0 | 3.0 | 3.1 |
| Annealed 650 K/100 h | 2.3 | 3.3 | 3.0 | 3.0 | 3.1 |
| Annealed 700 K/100 h | 2.1 | 3.3 | 2.7 | 2.7 | 3.0 |

sliding is the dominant deformation mechanism. This deformation mechanism is characterised by a high strain rate sensitivity of the flow stress. The strain rate sensitivity parameter $m$ measured in our material was found deeply below the bottom limit of superplasticity ($m = 0.3$). This result is not surprising as the tensile tests were performed at room temperature whereas superplastic behaviour of Al-based alloys is generally observed at temperatures above 700 K. A question arises whether the extruded powder material might exhibit superplastic characteristics if it is strained at higher temperatures. The results of these experiments will be published elsewhere.

## 5. Conclusions

1. High-energy gas atomisation does not enable preparation of a segregation free microstructure in the Al-1.2at.%(Zr+Ti) alloy. The level of supersaturation of the matrix by Zr and Ti atoms is significantly lower than that in the melt-spun ribbons of the same material.

2. Extrusion of the atomised powder material at temperatures 623 and 673 K results in a fine-grained structure (grain or subgrain size of the order of 1 $\mu$m). Coarse primary particles containing Fe and other impurities and coarse particles of the $L1_2$ modification of the $Al_3(Zr_xTi_{1-x})$ phase were observed. No fine particles of this phase arranged into a fan shaped configuration (typical of melt spun ribbons) were found.

3. The microhardness of the powder material is significantly lower than that of the as-melt spun material. The large size of particles in the powder material is the principal cause of this difference.

4. The ageing response both of the as-atomised and extruded powder materials is significantly lower than that in the as-melt-spun material. The reason might be the lower supersaturation of the matrix prior to ageing.

5. The long term stability of the microhardness is similar in both types of material. Overageing observed at 700 K is connected with the transformation of the $L1_2$ to $DO_{23}$ modification of the $Al_3(Zr_xTi_{1-x})$ phase. The fine grained microstructure is maintained even after ageing at 700 K.

6. A good correlation between the ultimate tensile strength and microhardness was found.

**Acknowledgements**

We would like to dedicate the paper to Professor Dr. Z. Trojanová on the occasion of her $60^{th}$ birthday. The authors are grateful to Dr. F. M. Knoop, TU Clausthal, Germany, for the preparation of the material and to M. Čepová for the help with processing of TEM micrographs. This work is a part of the research program MSM113200002 that is financed by the Ministry of Education, Youth and Sports of the Czech Republic within the framework of the Research Goal 190-01/206054. A partial support came from the Grant Agency of Charles University under the Contract No. 283.

## REFERENCES

[1] SRINIVASAN, S.—DESCH, P. B.—SCHWARTZ, R. B.: Scripta Metall., *25,* 1991, p. 2513.
[2] NES, E.: Acta Metall., *20,* 1972, p. 499.
[3] MONDOLFO, L. F.: Aluminium Alloys: Structure and Properties. London, Butterworth 1976.
[4] DAS, S. K.—DAVIS, L. A.: Mater. Sci. Eng., *98,* 1988, p. 1.
[5] LIFSHITZ, I. M.—SLYOZOV, V. V.: J. Phys. Chem. Solids, *19,* 1961, p. 35.
[6] WAGNER, C.: Z. Elektrochem., *65,* 1961, p. 581.
[7] ZEDALIS, M.—FINE, M. E.: Scripta Metall., *17,* 1983, p. 1247.
[8] ZEDALIS, M.—FINE, M. E.: Met. Trans. A, *17,* 1986, p. 2187.
[9] TSUNEKAWA, S.—FINE, M. E.: Scripta Metall., *16,* 1982, p. 391.
[10] NES, E.: Acta Metall., *20,* 1972, p. 499.
[11] JONES, H.: Rapid Solidification of Metals and Alloys. London, Inst. of Metallurgists 1982.
[12] MÁLEK, P.—BARTUŠKA, P.—PLEŠTIL, J.: Kovove Mater., *37,* 1999, p. 386.
[13] MÁLEK, P.—JANEČEK, M.—SMOLA, B.—BARTUŠKA, P.: Kovove Mater., *38,* 2000, p. 9.
[14] MÁLEK, P.—CHALUPA, B.—PLEŠTIL, J.: Kovove Mater., *38,* 2000, p. 77.
[15] MÁLEK, P.—JANEČEK, M.—SMOLA, B.: Kovove Mater., *38,* 2000, p. 160.
[16] OHASHI, T.—ICHIKAWA, R.: Met. Trans., *3,* 1972, p. 2300.
[17] NES, E.—BILLDAL, H.: Acta Metall., *25,* 1977, p. 1031.
[18] OHASHI, T.—ICHIKAWA, R.: Z. Metallkde., *61,* 1973, p. 517.
[19] HORI, S.—TAI, H.—NARITA, Y.: Microstructure of rapidly solidified Al-Ti alloys containing titanium up to 40 % and its thermal stability. In: Rapidly Quenched Metals. Eds.: Steeb, S., Warlimont, H. Elsevier Sci. Publ. 1985, p. 911.
[20] SHAW, M. C.: In: Mechanical Behavior of Materials. Eds.: McClintock, F. A., Argon, A. S. Addison/Wesley, Reading, MA 1966, p. 443.
[21] CAHOON, J. R.—BROUGHTON, W. H.—KUTZAK, A. R.: Metall. Trans., *2,* 1971, p. 1979.
[22] TABOR, D.: The Hardness of Metals. Oxford, Clarendon Press 1951, p. 1.
[23] EDINGTON, J. W.—MELTON, K. N.—CUTLER, C. P.: Prog. Mater. Sci., *21,* 1976, p. 61.

Received: 7.10.2002